Available online at www.sciencedirect.com
ScienceDirect
Journal of Sound and Vibration 311 (2008) 1213–1227
JOURNAL OF SOUND AND VIBRATION
www.elsevier.com/locate/jsvi

An improved transmission line matrix model for the 2D ideal wedge benchmark problem

I.J.G. Scott, D. de Cogan*,[1]

School of Computing Sciences, University of East Anglia, Norwich NR4 7TJ, UK

Received 7 May 2007; received in revised form 2 October 2007; accepted 4 October 2007
Available online 19 November 2007

Abstract

The numerical modelling of acoustic propagation in underwater environments using transmission line matrix (TLM) has received little attention for some time. This has been due, in part, to the need for an open boundary description, also known as a 'perfectly matched load' or PML, and the requirement for an accurate description of non-uniform bounding walls. The first of these problems has been solved by many researchers in subsequent years. The paper describes a novel solution to the second problem, allowing the incorporation of boundary-conforming Cartesian meshes into TLM schemes for acoustic propagation. This and a related technique are compared using the Buckingham and Tolstoy ideal 2D wedge benchmark test.

1. Introduction

Modelling of underwater acoustic propagation follows the conventional approach of:

- practical observations,
- mathematical equation which approximates observed behaviour,
- solve mathematical equation subject to initial/boundary conditions and assumptions.

Exact analytical solutions are rarely possible for complex geometries and recourse is made to numerical methods. Even here it is usual to take the underlying partial differential equation (PDE) and to solve it using techniques such as finite differences. It could well be argued that such an approach involves two levels of approximation. Transmission line matrix (TLM) represents an alternative approach in that the physical problem is modelled by an electric circuit analogue which can be solved exactly. There is one approximation, the extent to which the analogue matches the physical problem. What makes TLM different from other circuit analogue techniques is the use of transmission lines. These have distributed electrical parameters and as a consequence they introduce time-delay, so that both space and time are discretised. This has the potential of permitting the modeller to treat each discrete position in space (node) in isolation from all others at any

*Corresponding author.
E-mail address: ddc@cmp.uea.ac.uk (D. de Cogan).
[1]D. de Cogan retired from UEA and is currently teaching at SBC/USST, Shanghai, PRC.

0022-460X/$ - see front matter © 2007 Elsevier Ltd. All rights reserved.
doi:10.1016/j.jsv.2007.10.009

instant in time on the basis that it takes the discretisation time interval for information to be communicated between neighbours. This also allows the use of heavily optimised code to exploit the natural parallel configuration of the problem space. The technique was originally developed [1] to solve propagation problems in electromagnetic waveguides. Saleh and Blanchfield [2] applied it to acoustic propagation in air and the first applications in underwater acoustics were reported by Coates et al. [3]. This work was detailed by Willison [4] whose Ph.D. thesis included the first investigation using the Buckingham and Tolstoy [5] benchmark test and TLM. Some earlier work on the problem proposed by Buckingham and Tolstoy [5] was reported in Refs. [6–8]. These papers were aimed specifically at solving the problem of Ref. [5], and as such do not adapt well to other areas of use with the exception of Ref. [7]. The method proposed in Ref. [7] is similar in nature to our approach here, but lacks the benefit of a boundary conforming scheme inevitably introducing errors from the sloping surface of the wedge. The method we will propose in this paper is much more general, and can as such be used in a variety of applications.

Willison also highlighted some of the difficulties in the further exploitation of TLM in this area. Chief amongst these was the numerical load which was imposed by the dispersive effects of using a discretised mesh. Further progress was unlikely unless a broad-band perfectly matched terminating boundary could be developed. Such problems had already been highlighted by Arnold et al. [9]. This issue has now been resolved [10]. Willison's Ph.D. research had originally intended to model the influence of surface condition on multi-path acoustic propagation in a shallow water channel and copious experimental measurements had been made on the effect of wave-height in the lake (broad) on the University of East Anglia Norwich campus. However, the scale of discretisation that was required to 'accurately' model the water/air interface within a wave using a step-wise approximation was prohibitive and there the matter rested.

In the interim, several authors have looked at techniques for surface conforming meshes within TLM numerical schemes. One of the major difficulties is the requirement for synchronous arrival of signals, which at the least, requires that there is a distance Δx between nodes (measurement points within the problem space) and a distance $\Delta x/2$ from a node to a boundary, where Δx is the spatial discretisation of the model. The interface between meshed space and a real boundary cannot be subjected to this restriction as the real boundary often will not fall on an exact integer multiple of $\Delta x/2$, this problem is illustrated in Fig. 1, for a mesh size of $N \times N$ nodes and sampling discretisation Δx. The total size modelled is hence $N\Delta x$ units. The scheme due to Mueller et al. [11] is the most successful at placing boundaries in arbitrary locations that do not fall in steps of $\Delta x/2$ in the TLM mesh. Their approach does however have a computational overhead. This paper reports on an alternative approach which does not involve the recursion that is inherent in the Mueller algorithm. Comparisons are made between these two techniques and a 'normal' stepped boundary approach, using the Buckingham and Tolstoy wedge as a benchmark. This problem involves a sloping pressure release boundary representing the sea floor and an equivalent flat boundary for the sea–air interface. While this is obviously not an accurate interpretation of the real situation and is probably why the benchmark has had

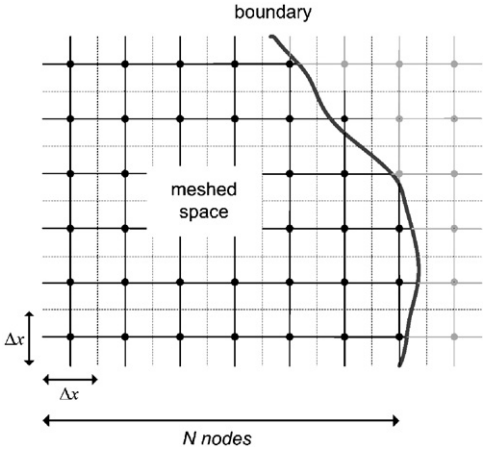

Fig. 1. Meshed space interfacing with fixed boundary. Mesh discretisation definition is also illustrated.

limited popularity, the problem does give an ideal situation with which to test a boundary conforming scheme. TLM has not been widely used in underwater acoustics mainly due to the need for this accurate boundary description. Finite differences (FD) on the other hand does not suffer from this problem, and has hence received much greater interest. However, with the boundary conforming approach proposed in this paper, and the simplicity of the TLM method, we now believe the TLM approach is at a level equivalent to FD for use in acoustic modelling.

The paper will begin with a summary of transmission line theory, highlighting the areas specific to the current situation. We will develop this to illustrate how the TLM method is formed in 2D. A more in-depth analysis and discussion can be found in Refs. [10, pp. 9–85,12]. We will give a comparison of the boundary conforming scheme proposed in this paper against another popular scheme proposed in Ref. [11], and compare both to a 'normal' stepped boundary description. The paper will conclude with a short summary of the points raised in the paper. The paper aims to introduce the TLM method to a largely acoustics audience, while treating a benchmark problem illustrating the benefit of the new boundary conforming method that is proposed. It should be noted that the introduction to transmission line theory which is given here is only a brief overview of a wide and diverse field. For a better understanding of TLM and why it is possible to describe physical problems using transmission line analogies the reader is encouraged to consult the relevant resources, Refs. [13,14] are recommended for first reading.

2. Transmission lines and transmission line matrix modelling

In describing transmission line behaviour there are many possible levels of abstraction. However, in electrical analogue terms we treat them as having a string of inductances in series and a ladder of capacitances in parallel. The former acts as a store of magnetic energy (kinetic energy in mechanical terms), while the latter stores electrical energy (potential energy in mechanics). The value of inductance is generally quoted per unit length as L_d, while the equivalent value of capacitance per unit length is designated as C_d. The ratio L_d/C_d is a constant for a given transmission line of uniform constituents and geometry. The square root of this ratio is defined as the impedance Z, and is independent of length. The product of L_d and C_d has dimensions (time^2−distance^{-2}) and indeed we can write an expression for the propagation velocity of a signal on a transmission line as

$$v = \frac{1}{\sqrt{L_d C_d}}. \tag{1}$$

If this is used together with the definition for impedance, we arrive at two very useful expressions for the time, Δt, it takes a signal to travel a specific distance, Δx, as a function of one or other of the line parameters:

$$\Delta t = Z C_d \Delta x \quad \text{or} \quad \Delta t = \frac{L_d \Delta x}{Z}. \tag{2}$$

Strictly speaking these are valid only as limiting relationships at low frequencies or long wavelengths, but if Δx is at least one order of magnitude smaller than the shortest wavelength of interest, they give good numerical accuracy.

So long as the impedance of a transmission line is uniform then signals in transit suffer no attenuation or dispersion. However, if the impedance changes at some location, then there will be reflections and transmissions. Thus, when an impulsive signal travelling on a line of impedance Z_A encounters a change of line impedance to Z_B, this will cause part of the signal to be reflected and part to be transmitted. The reflection and transmission coefficients are:

$$\rho = \frac{Z_B - Z_A}{Z_B + Z_A} \quad \text{and} \quad \tau = \frac{1-\rho}{3}, \tag{3}$$

respectively for 2D.

This applies regardless of whether we are considering the voltage or the current component of the signal. The treatment which is given here could be done for current or voltage pulses. In common with most works on the subject we will use a voltage-based analysis. It will be for propagation in two dimensions.

Note the use of the points of the compass which are used to designate direction. In Fig. 2 we see a signal ${}^iV_W$, (voltage pulse incident from the west) and as it arrives at the node it sees three impedances ahead of it. As it has no knowledge of their physical length, it assumes that they are infinitely long and hence it sees a load impedance $Z/3$. Using Eq. (3) we have the following scattering parameters:

$$\rho = \frac{Z/3 - Z}{Z/3 + Z} = -\frac{1}{2} \quad \text{and} \quad \tau = \frac{1-\rho}{3} = \frac{1}{2}. \tag{4}$$

We see that $\rho + 3\tau = 1$ and that $\rho^2 + 3\tau^2 = 1$, the latter represents the conservation of energy.

At the same time as the signal is coming in from the west, there are other signals incident from the north, south and east. The potential at the node is a superposition, i.e. the sum of the currents divided by the sum of the admittances

$$k\phi(x, y) = \frac{\sum I}{\sum Y} = \frac{\left[2^iV_N/Z + 2^iV_S/Z + 2^iV_E/Z + 2^iV_W/Z\right]}{\left[1/Z + 1/Z + 1/Z + 1/Z\right]}$$

or

$$k\phi(x, y) = \frac{\left[{}^iV_N + {}^iV_S + {}^iV_E + {}^iV_W\right]}{2}. \tag{5}$$

These signals then scatter and head off as scattered pulses. Thus what came in from the west is reflected to the west and transmitted to the north, south and east. This is summarised as

$$\begin{pmatrix} {}^sV_N \\ {}^sV_S \\ {}^sV_E \\ {}^sV_W \end{pmatrix} = \frac{1}{2}\begin{pmatrix} -1 & 1 & 1 & 1 \\ 1 & -1 & 1 & 1 \\ 1 & 1 & -1 & 1 \\ 1 & 1 & 1 & -1 \end{pmatrix}\begin{pmatrix} {}^iV_N \\ {}^iV_S \\ {}^iV_E \\ {}^iV_W \end{pmatrix}. \tag{6}$$

This is the *Scattering Rule* in our algorithm.

Each pulse travels the discretisation distance Δx during the discretisation time Δt after which it becomes an incident pulse at an adjacent node. The connections to other nodes as seen at node (x, y) can be expressed in terms of space and time-step, $k+1$ as

$$\begin{aligned} k+1{}^iV_N(x, y) &= k^sV_S(x, y+1), \\ k+1{}^iV_S(x, y) &= k^sV_N(x, y-1), \\ k+1{}^iV_E(x, y) &= k^sV_W(x+1, y), \\ k+1{}^iV_W(x, y) &= k^sV_E(x-1, y), \end{aligned} \tag{7}$$

i.e. the new incident voltage on the North line of node (x, y) is the scattered voltage on the South line from the node above, etc. This is the *Incidence Rule* in our algorithm.

A TLM scheme comprises the repeated application of theses two rules for every node in our space. Time advances by Δt every time we repeat this automaton. We can at any time, $k\,\Delta t$ inspect the potential at each node by using Eq. (5).

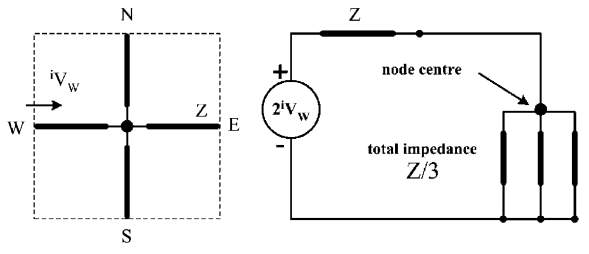

Fig. 2. A 2D TLM node and its Thévenin equivalent circuit representation.

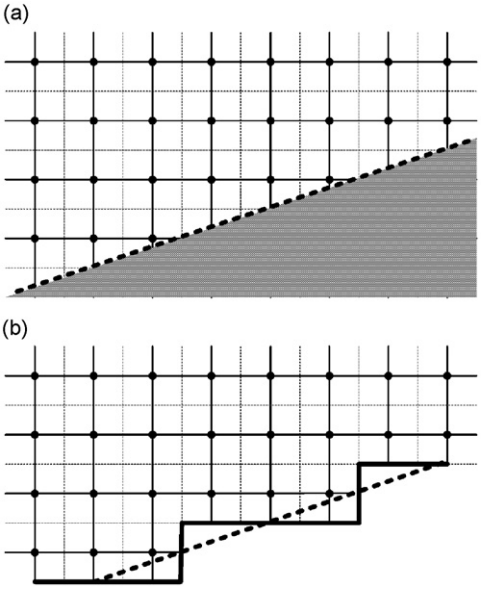

Fig. 3. A 2D assembly of the components in Fig. 1, viewed from above with (a) a sloping boundary and (b) a step-wise approximation to the sloping boundary. The dashed lines show the frontiers between nodes.

As the reader is probably aware by now, depending on the propagation angle of a wave within the mesh, relative dispersion errors will become a problem. TLM supports vertical and horizontal propagation with no error. Diagonal directions will suffer some form of dispersion, it is reported in Ref. [12] this dispersion can be minimised providing $\Delta x < \lambda/10$, i.e. there must be a minimum of 10 sample points within one wavelength of the primary frequency of excitation.

2.1. Boundaries

In conventional TLM a boundary ($\rho = 1$ for rigid[2] and $\rho = -1$ for pressure release[3]) is placed at a distance $\Delta x/2$ beyond the nearest node. A signal leaving the node travels during time $\Delta t/2$ where it is reflected (in-phase for $\rho = 1$ and in anti-phase for $\rho = -1$). It then travels back to the node during the remaining interval $\Delta t/2$, so that it arrives back at the same time as all other signals in the network arrive at their destinations. This is fine so long as the boundary conforms to a Cartesian mesh, as was the case in the model for an electromagnetic waveguide by Johns and Beurle [1]. However, if this is not the case, as in the sloped boundary of Fig. 3(a), then we could use a step-wise approximation as shown in Fig. 3(b).

This representation is computationally cheap and avoids the complexities often found in other techniques which approximate the arbitrary boundaries of the mesh more closely. However, the errors introduced by the stepped formulation can often lead to largely inaccurate results. The alternative is to use either local or general refinement of the mesh, i.e. using a smaller spatial discretisation, Δx. Although this is an acceptable approach and widely used, the memory and time requirements of the algorithm increase dramatically, often causing the model to become unsolvable within reasonable computational time-scales.

Fig. 4 shows a bounding surface of the computation space crossing between the start and finish points of the transmission line section, as the length l_A is not an integer multiple of $\Delta x/2$ this cannot be included in the algorithm directly. For example, a signal travelling along the line of length l_A will reach the bounding surface and reflect back at a time less than $(k+1)\Delta t$, where k is the current time step. The same signal travelling along the line of length $\Delta x/2$ will reach the bounding surface at time $(k+1/2)\Delta t$, reflecting back and reach the node again at exactly $(k+1)\Delta t$. As all signals propagating in TLM must scatter and become incident at all nodes at

[2]Sometimes called a 'mirror' boundary. Current/displacement is zero, voltage/pressure is maximum.
[3]In electrical terms the voltage at such a boundary is zero, and the current is a maximum.

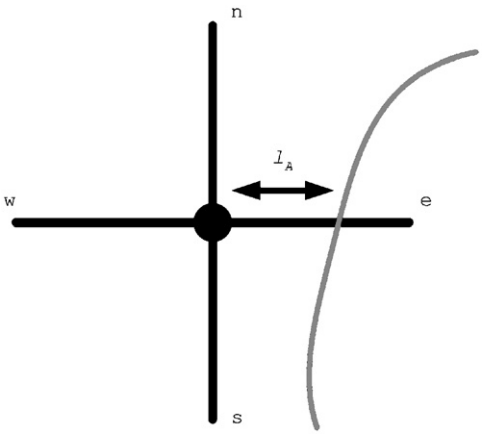

Fig. 4. Bounding wall at non-discrete multiple of models discretisation.

the same time, the system cannot be modelled as it is currently shown. The section which follows will outline one of the best techniques currently available for addressing this problem.

3. Introduction to the MBH conforming boundary technique

The technique due to Mueller et al. [11], hereafter referred to as the MBH method suggests locating a reference plane at a distance $\Delta x/2$ from the node. The arbitrary perfectly reflecting boundaries of the mesh are then defined recursively as

$$ {}_kV^i = \rho\frac{1-\kappa}{1+\kappa}{}_kV^r + \frac{\kappa}{1+\kappa}(\rho_{k-1}V^r + {}_{k-1}V^i), \tag{8}$$

where ${}_{k-1}V^i$ and ${}_{k-1}V^r$ represent the incident and reflected (scattered) pulses at time $k-1$, respectively. The reflection coefficient ρ, will be set at -1 for the purposes of this paper. κ is defined to be $\sqrt{2l/\Delta x}$. This scheme takes a proportion of the incident and reflected pulses from the previous time step and adds it to the current reflected pulse. While this formulation provides a closer approximation to the bounding surfaces of the TLM mesh than a stepped approximation can, it contains two shortfalls not inherent in the stepped description. One immediate problem is the recursion that must be applied at every node at every discrete time step. The extra matrices that require storage space, approximately double the memory requirements of the algorithm. Advanced techniques can be utilised to reduce this memory 'footprint' however, the complexity of the algorithm is increased further.

Secondly, inspection of Fig. 5 shows that the bounding surface crosses after the $\Delta x/2$ line end. In the MBH description this is the only crossing possible. This imposes a constraint on the exact formulation of the mesh, requiring further information to be lost if the boundary crosses before $\Delta x/2$. It is necessary to remove the boundary adjacent node, extending the lines from the neighbouring nodes to account for the missing node. Analysis of this situation is performed in Ref. [11], ensuring the system remains stable. In the modelling performed in Section 4 of this paper, we see that the missing nodes do not appear to inhibit the results drastically.

4. Improved conforming boundary description

The description we propose to model the arbitrary placed boundaries of the TLM mesh, performs an impedance transformation on transmission line segments of boundary adjacent nodes. Details of its use and validation for an electromagnetic simulation can be found in Ref. [15]. An example of another problem solved using this boundary conforming scheme can be found in Ref. [16].

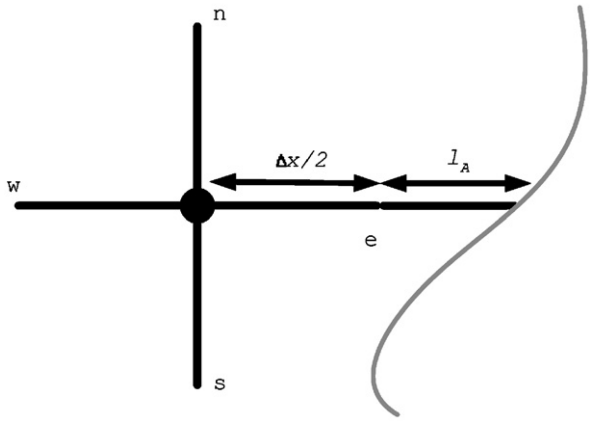

Fig. 5. MBH model of non-discrete bounding wall placement.

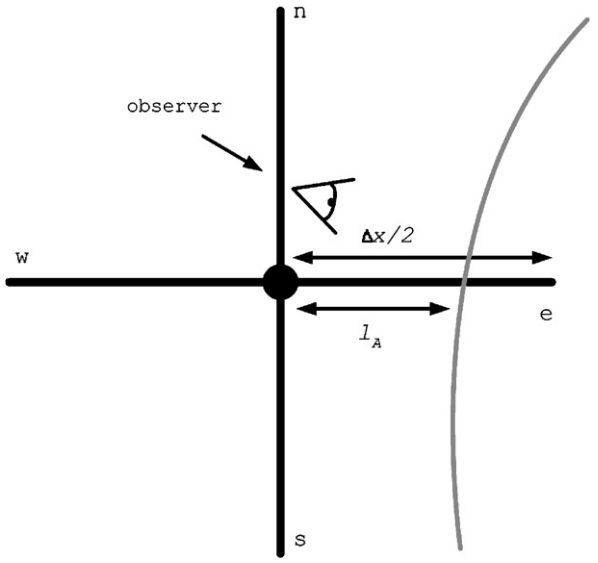

Fig. 6. Impedance of the line, including the termination as observed from the boundary adjacent node.

In this method we consider a boundary-adjacent node where we place an observer at the node looking down the transmission line towards the boundary. Although this might appear to be a simple change, it removes the need for recursion, eliminating some of the problems of the MBH method while obtaining results of considerable improvement. The observed impedance of a line of length l_A and intrinsic impedance Z with a terminating impedance Z_L is given from the point of view of the observer (Fig. 6) as

$$Z_{\text{obs}} = Z\left[\frac{Z_L + Z\,\tanh(\beta l_A)}{Z + Z_L\,\tanh(\beta l_A)}\right], \tag{9}$$

where $\beta = 2\pi/\lambda$, (λ is the wavelength).

Using the low-frequency approximation which is a cornerstone of TLM, the intrinsic impedance Z of the line can be expressed in terms of the distributed capacitance as well as the spatial and temporal discretisations

of the model (Δx and Δt):

$$Z = \frac{\Delta t/2}{C_d \Delta x/2}. \tag{10}$$

It can also be expressed in terms of C_d and $\Delta t'$, the time it would take to traverse the line of length l_A to the boundary, $Z = \Delta t'/C_d l_A$.

This implies that we could replace the line of length l_A with another line of length $\Delta x/2$ adjusting the impedance to compensate for the adjusted length, while causing the signal to now arrive back at the node at an integer multiple of $\Delta t/2$. It is this impedance transformation that is the basis of our approach.

For the case when $\rho = 1$ (i.e. $Z_L \to \infty$, a rigid boundary in acoustics), the formulation given in Eq. (9) can be simplified, to give before and after transformation:

$$Z_{\text{obs}} = \frac{Z}{\tanh(\beta l_A)} \quad \text{before,} \tag{11a}$$

$$Z_{\text{obs}} = \frac{Z_A}{\tanh(\beta \Delta x/2)} \quad \text{after,} \tag{11b}$$

therefore the line of length $\Delta x/2$ of the transformed impedance, Z_A, appears identical to the observer at the node.

If we assume low frequencies within the mesh then $\tanh(\beta \Delta x/2)$ can be replaced with $\beta \Delta x/2$, giving

$$Z_{\text{obs}} = \frac{Z_A}{\beta \Delta x/2}. \tag{12}$$

Equating the RHS before and after transformation in Eqs. (11a) and (11b), and making the same assumption of low frequencies, so $\tanh(\beta l_A)$ can be replaced with βl_A, gives

$$\frac{Z}{\beta l_A} = \frac{Z_A}{\beta \Delta x/2} \tag{13a}$$

rearranging this gives

$$Z_A = Z\left[\frac{\Delta x}{2 l_A}\right]. \tag{13b}$$

If we undertake the same analysis for a pressure release boundary (i.e. $Z_L \to 0$ so that $\rho = -1$) Eq. (11) in the before and after transformation formulation gives

$$Z_{\text{obs}} = Z \tanh(\beta l_A) \quad \text{or} \quad Z_{\text{obs}} = Z_A \tanh(\beta \Delta x/2). \tag{14}$$

Proceeding as before we obtain

$$Z_A = Z\left[\frac{2 l_A}{\Delta x}\right]. \tag{15}$$

If these transformations for pressure release boundaries of arbitrary shape at arbitrary locations around a TLM mesh are made, we will show that we can match well-known analytical results. The scheme provides an accurate description of the bounding walls of a TLM mesh, while ensuring that all pulses within the computation space remain in synchronisation with one another. This technique will be termed Uniform method in the remainder of this paper.

5. Model comparisons

5.1. Analytical solution

To test the viability of our proposal, the benchmark acoustic problem known as the *Buckingham and Tolstoy wedge* [5] has been implemented. The model represents a 2D underwater continental slope, with ideal pressure release boundaries at the air–sea and sea–soil interfaces. Fig. 7 illustrates the coordinate system used

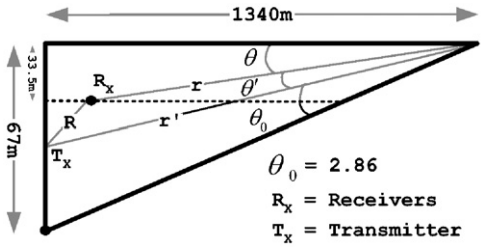

Fig. 7. Coordinate system of Buckingham and Tolstoy acoustic wedge.

in the formula:

$$\phi = \frac{\mathrm{j}\pi}{\theta_0}\sum_{m=1}^{\infty} J_v(kr_<)H_v^{(1)}(kr_>)\,\sin(v\theta)\,\sin(v\theta'), \tag{16}$$

where J_v is the Bessel function of the first kind of order v, $H_v^{(1)}$ is the Hankel function of the first kind of order v, $r_< = \min(r, r')$, $r_> = \max(r, r')$ and $v = m\pi/\theta_0$. Eq. (16) is used to describe the acoustic field evident within the wedge. In the implementation performed here the summation is run to 100. In Ref. [5] an analysis is performed to ensure the results obtained are as accurate as possible. The input frequency for the calculations performed here is set at 75 Hz and the source is placed at the mouth of the wedge (as shown in Fig. 7), the size of the wedge has been adjusted to replicate those of Ref. [5] almost exactly. We have the addition of a centre node in the vertical direction to allow the source to be placed at the centre of the 'mouth' of the wedge. This creates a slight discrepancy between our analytical results and those of Ref. [5], however this allows a closer comparison with the numerical models. To allow Δx to be set to 1, and hence obtain a fine mesh with a reasonable number of nodes, we have approximately scaled the problem by a factor of $\frac{1}{3}$ (with the addition of the centre node). The speed of sound in water is set at 1500 m/s. The normalised field in the wedge is calculated using Eq. (16) as

$$A = \frac{|\phi|}{|\zeta(1)|}, \tag{17}$$

where

$$\zeta(R) = (\mathrm{j}/4)H_0^{(1)}(kR) \tag{18}$$

and $H_0^{(1)}$ is the Hankel function of the first kind of order 0.

The results from Ref. [5] were replicated (with the slight change in dimensions) using Eqs. (16)–(18) in order to provide a benchmark against which to compare our three TLM simulations. Fig. 8 shows the full 2D surface of the wedge while Fig. 9 shows minus transmission loss in dB (as performed in Ref. [5]) as a function of range from source, calculated as

$$L = 20\log_{10}(A). \tag{19}$$

It can be observed from Fig. 8, as the input signal propagates up towards the apex of the wedge, the modes of the input signal begin to cut-off, until only one mode is supported close to the apex. This is illustrated more clearly in Fig. 9, showing how the transmission loss patterns contain rapid spatial fluctuations closer to the mouth of the wedge (as the signal is composed of multiple modes), stabilising to produce a smoothed pattern after 740 m (where only one mode comprises the transmission loss). The depth of receivers (10 m in this case), is chosen to coincide with the cut-off of the final mode, ensuring the receivers are outside the wedge when the water is too shallow to support even the lowest order mode.

Due to the 'brittleness' of this benchmark it is not as widely used as one would expect. The adjustment of the wedge dimensions and input frequency performed here is designed to match those of Ref. [5] almost exactly, and as can be seen, with the minor inclusion of a centre vertical node, the results differ from those of Ref. [5]

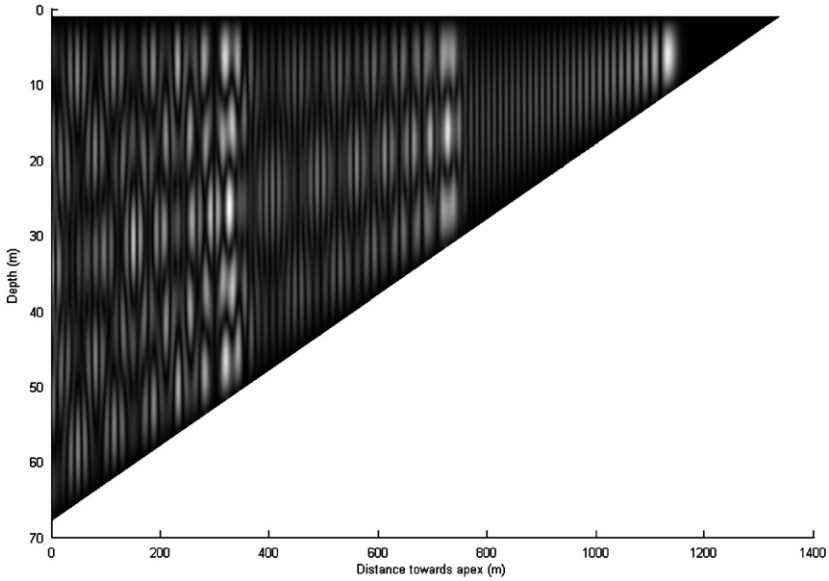

Fig. 8. 2D surface plot showing modes propagating in underwater acoustic wedge environment (analytical solution).

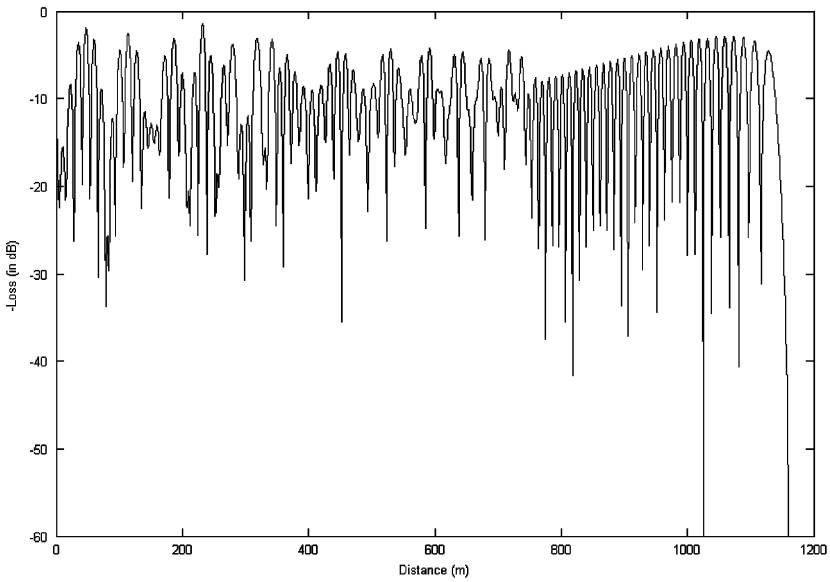

Fig. 9. Negative transmission loss as function of range from source in underwater acoustic wedge environment (analytical solution).

by a noticeable amount. We found that if the dimensions or input are adjusted, only slightly, then the results are changed considerably.

5.2. Stepped boundary model

The first numerical model that is presented is the stepped formulation that was described above. We have used a boundary reflection coefficient of $\rho = -1$ and have placed a sinusoidal continuous-wave point-source halfway down the mouth of the wedge. This injects at a frequency equal to that of the analytical solution, however as we are working in the time domain, it is necessary to run the simulation for long enough to allow the standing modes to appear. In the experiments performed, we find that a runtime of 85,000 iterations

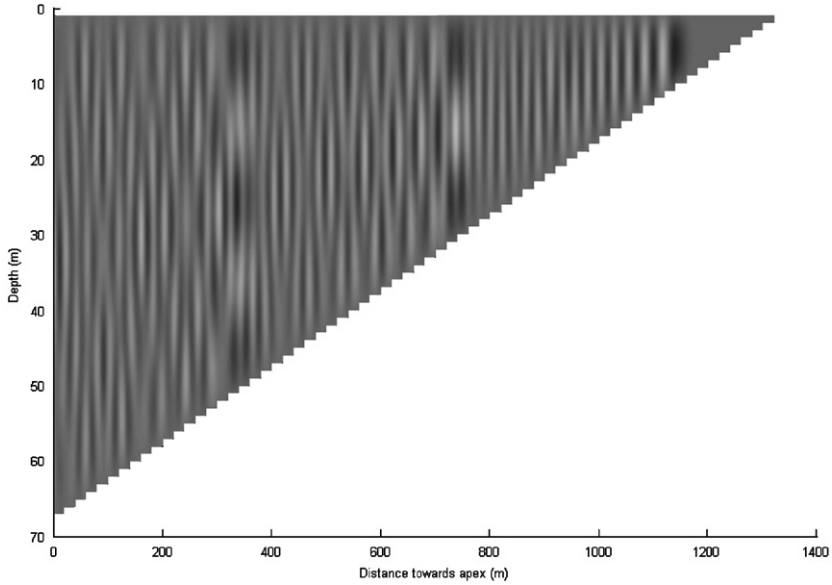

Fig. 10. 2D surface plot showing modes propagating in underwater acoustic wedge environment (stepped TLM solution).

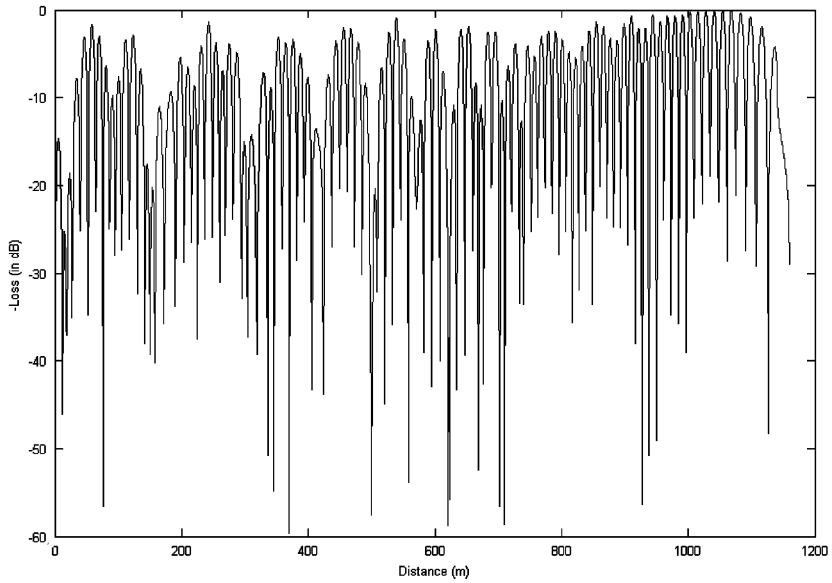

Fig. 11. Negative transmission loss as function of range from source, (stepped TLM solution).

(time steps of Δt) is sufficient enough to allow the injected wave to travel back and forth along the wedge and set up the standing waves, i.e. until steady state is reached. The resulting surface and transmission loss plots are shown in Figs. 10 and 11, respectively, where Fig. 10 has been calculated using Eq. (5) across each of the nodes on the surface of the wedge. As expected these are largely inaccurate, with spatial fluctuations being observed in the transmission loss patterns after the 740 m cut-off of the three modes. These inaccuracies are raised due to the stepwise nature of the sloping pressure release boundary, creating spurious waves opposing the propagating wave. The perfectly matched load absorber (PML) in all the TLM solutions is placed 30 nodes away from the mouth of the wedge, which inhibits the effect on the propagating signal. The PML acts as an absorber, to allow the model to believe there is a section of continuous ocean behind the wedge, this is needed

in all of the numerical models performed in this paper, details on the PML and subsequent analysis can be found in Ref. [12]. If we compare the accuracy of this stepped formulation with that of the analytical result of Fig. 9, the loss of fine detail is clearly visible, apparently swamped by errors from the stepped sloping boundary, (we expect a small error from the PML, however this is known to be insignificant in comparison to that from the boundary description).

5.3. MBH model

In this set of experiments we repeated the simulation but define the sloping boundary using the recursive approach due to Mueller et al. [11]. This allows the true location of the sloping walls between nodes to be described more accurately. The results are shown in Figs. 12 and 13, respectively. It is quite clear that there is a considerable improvement after the third mode is cut-off at 740 m. While the spatial fluctuations are still in phase with those of the stepped version, the amplitude of each is greatly reduced, creating a pattern that matches the analytical result much more closely. While this is greatly improved, the computational load increases drastically due to the recursive nature of the boundary definitions.

5.4. Uniform boundary model

Implementing the technique proposed in this paper, produces the results of Figs. 14 and 15, respectively. It can immediately be observed from the transmission loss in comparison to both the stepped and MBH solutions, the apparent lack of spatial fluctuations after the third mode is cut-off at 740 m greatly increases accuracy, in fact, ignoring the amplitude differences, the uniform results after 740 m match those of the analytical solution almost exactly. We note before 740 m, there is little improvement in accuracy, this can also be seen in the MBH solution. To show the likeness between the boundary conforming scheme approach and the analytical model, the plots of Figs. 9, 11, 13 and 15 have been separately normalised to fall between 0 and 1 dB, and the differences of the numerical models against the analytical are then plotted in Fig. 16, this shows the improved match in shape between analytical and Uniform, while ignoring the amplitude differences. The mesh used here was fairly fine and had Δx of 1, it would be easier to reduce this, making the mesh finer still, using the boundary conforming scheme proposed here, than it would using the MBH approach. The reduced memory requirements of the new technique, allow more memory to be left for the nodes within the mesh, while already achieving accuracy inline with the MBH approach.

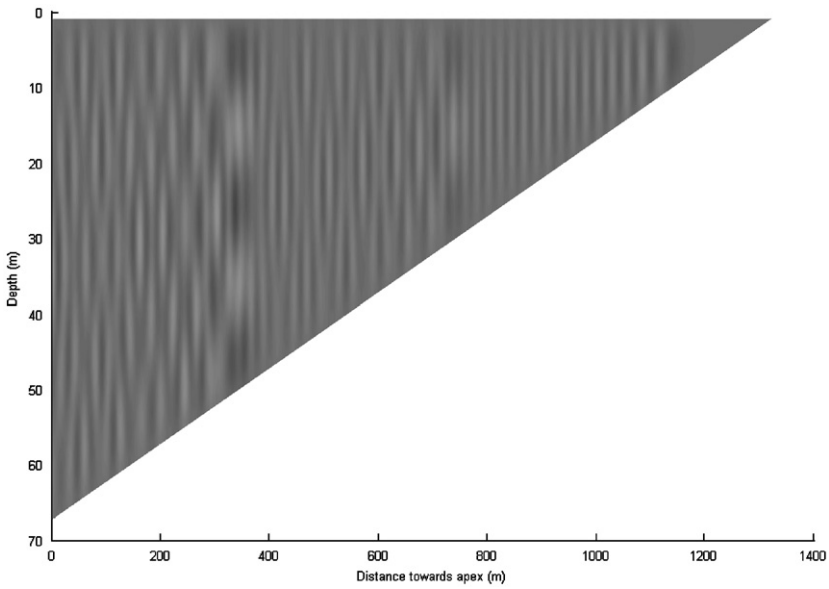

Fig. 12. 2D surface plot showing modes propagating in underwater acoustic wedge environment (MBH TLM solution).

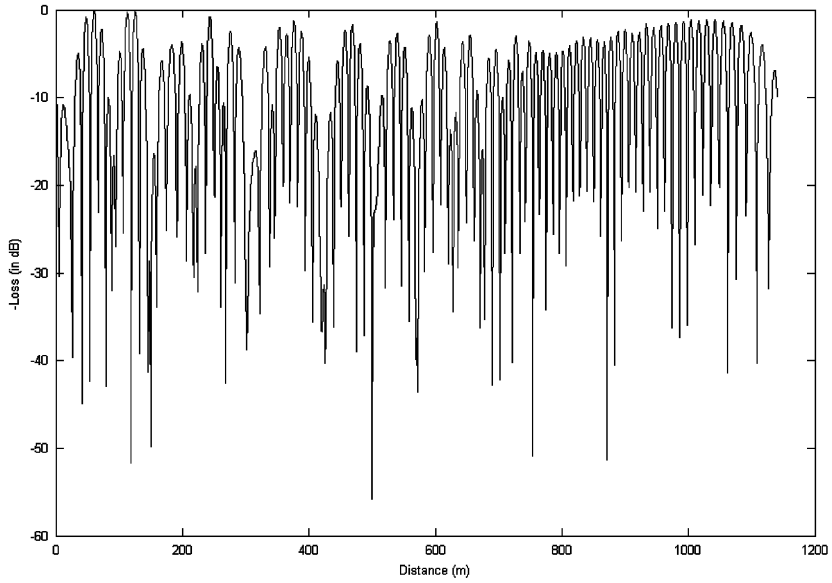

Fig. 13. Negative transmission loss as function of range from source in the (MBH TLM solution).

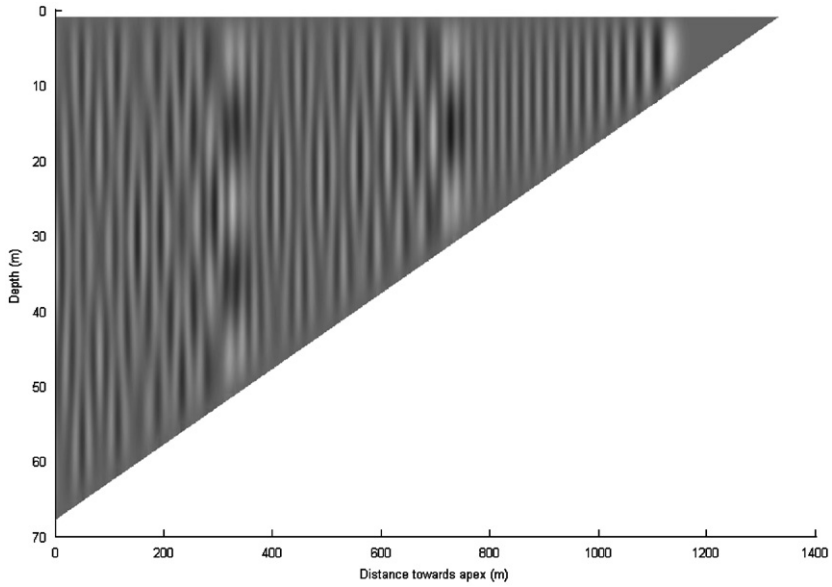

Fig. 14. 2D surface plot showing modes propagating in underwater acoustic wedge environment (Uniform TLM solution).

6. Conclusion

In this paper, we propose a novel solution to the placement of arbitrary boundaries in a TLM numerical model. While other numerical techniques (FD for example) are able to define arbitrary placed boundaries that do not fall on exact multiples of the models discretisation, until recently TLM generally was lacking in this capability in terms of an efficient algorithm.

We continued to validate the boundary conforming scheme, using the Buckingham and Tolstoy ideal 2D wedge benchmark test, a challenging problem which attempts to show the accuracy which is now obtainable

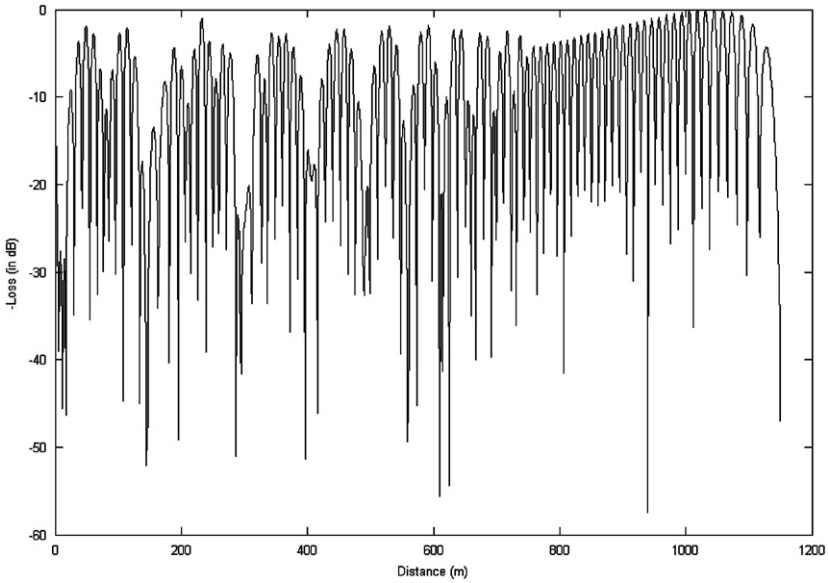

Fig. 15. Negative transmission loss as function of range from source (Uniform TLM solution).

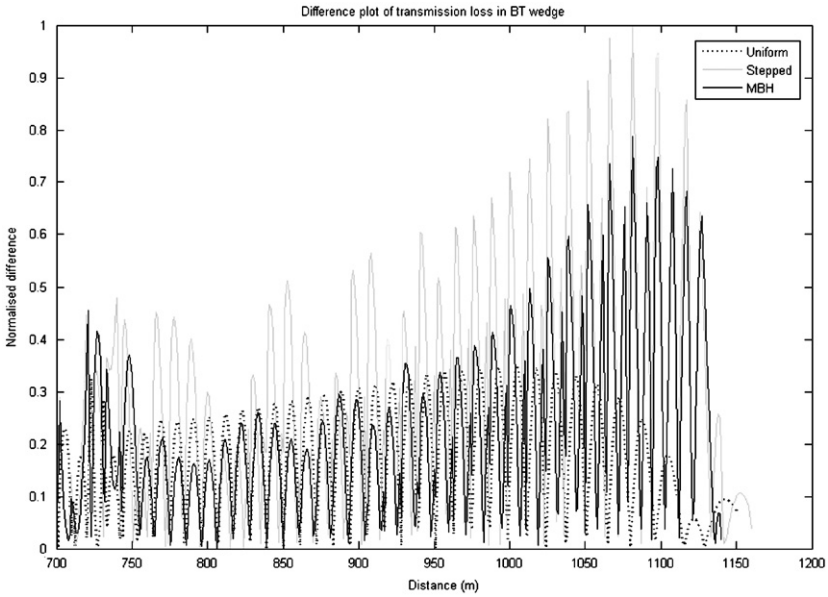

Fig. 16. Normalised difference of the three TLM numerical solutions against the analytical prediction. Difference is from transmission loss graphs in Figs. 11, 13 and 15 against the analytical result of Fig. 9.

using the boundary conforming description that is proposed. For this reason we would not expect an exact match between our numerical simulations, and that of the analytical solution, however we would still expect to notice a considerable increase in accuracy. This is shown in the two simulations attempting to better describe the boundaries. More complex TLM schemes are possible, which are slightly better adapted to modelling boundaries, however for ease of implementation and computational efficiency, the Cartesian TLM method is the most widely used. The boundary conforming scheme proposed here attempts to keep the computational efficiency and simplicity of the stepped TLM method while also improving the accuracy.

Acknowledgment

The authors would like to acknowledge the assistance and many useful comments which have been provided by Dr. J. Flint, Loughborough University, UK.

References

[1] P.B. Johns, R.L. Beurle, Numerical solution of 2-dimensional scattering problems using a transmission line matrix, *Proceedings of the IEE* 118 (1971) 1203–1208.
[2] A. Saleh, P. Blanchfield, Analysis of acoustic radiation patterns of array transducers using the TLM method, *International Journal of Numerical Modelling* 3 (1990) 39–56.
[3] R.F.W. Coates, D. de Cogan, P. Willison, Transmission line matrix modelling applied to problems in underwater acoustics, *Proceedings of International Oceans Conference*, Washington, DC, September '90.
[4] P.A. Willison, Transmission Line Matrix Modelling of Underwater Acoustic Propagation, PhD Thesis, University of East Anglia, Norwich, 1992.
[5] M.J. Buckingham, A. Tolstoy, An analytical solution of benchmark problem 1: the 'ideal' wedge, *Journal of the Acoustical Society of America* 87 (1990) 1511–1513.
[6] F.B. Jensen, C.M. Ferla, Numerical solutions of range-dependant benchmark problems in ocean acoustics, *Journal of the Acoustical Society of America* 87(4) 1499–1510.
[7] R.A. Stephen, Solutions to range-dependant benchmark problems by the finite-difference method, *Journal of the Acoustical Society of America* 87(4) 1527–1534.
[8] M.D. Collins, Benchmark calculations for higher-order parabolic equations, *Journal of the Acoustical Society of America* 87(4) 1535–1538.
[9] E.A. Orme, P.B. Johns, J.M. Arnold, A hybrid modelling technique for underwater acoustic scattering, *International Journal of Numerical Modelling* 1 (1998) 189–206.
[10] D. de Cogan, W.J. O'Connor, S. Pulko, *Transmission Line Matrix Modelling in Computational Mechanics*, Taylor & Francis, CRC Press, London, 2006, pp. 74–85.
[11] U. Mueller, A. Beyer, W.J.R. Hoefer, Moving boundaries in 2-D and 3-D TLM simulations realized by recursive formulas, *IEEE Trans. on Micro. Theo. and Tech.* 40 (12) (1992) 2267–2271.
[12] C. Christopoulos, *The Transmission Line Modelling Method*, OUP/IEEE Press, 1995.
[13] D.K. Cheng, *Field and Wave Electromagnetics*, Addison-Wesley, Reading, MA, 1989.
[14] J.D. Kraus, D.A. Fleisch, *Electromagnetics with Applications*, fifth ed., McGraw-Hill, New York, 1999.
[15] I.J.G. Scott, D. de Cogan, *Improved Mesh Conforming Boundaries for the TLM Numerical Method, PIERS (Progress in Electromagnetics Research Symposium)*, Cambridge University Press, Cambridge, MA, 2006, pp. 336–343.
[16] I. J. G. Scott, D. de Cogan, Acoustic wave propagation in underwater shallow channel environments, *Proceedings of IEEE Oceans 07*, Aberdeen, Scotland, June 2007.